Phase-offset frequency stabilization of a diode laser for ytterbium quantum optics experiments

Clara Marie Witte

Bachelorarbeit in Physik
angefertigt im Institut für Angewandte Physik

vorgelegt der
Mathematisch-Naturwissenschaftlichen Fakultät
der
Rheinischen Friedrich-Wilhelms-Universität
Bonn

January 2025

Ich versichere, dass ich diese Arbeit selbstständig verfasst und keine anderen als die angegebenen Quellen und Hilfsmittel benutzt sowie die Zitate kenntlich gemacht habe.

Bonn, ... 22. Januar 2025 ....
Datum   Unterschrift

1. Gutachter: Prof. Dr. Sebastian Hofferberth
2. Gutachter: Dr. Frank Vewinger

Contents

Introduction

With the introduction of the first ruby laser in 1960 and the helium-neon laser in 1962 [1], lasers have become an integral part not only of scientific research but also of everyday life. The variety of lasers has increased significantly with the usage of different wavelengths and active mediums; be it for high precision measurements, laser microscopy in biology or eye-diagnostics in medicine [2]. Commonly used lasers are solid-state, dye and semiconductor lasers [1].

Not only has the variety of lasers expanded over the years, but so have the possibilities for their use in scientific research. The Nonlinear Quantum Optics (NQO) group at the University of Bonn, for example, uses lasers to trap and cool atoms in a magneto-optical trap (MOT). These MOTs are used to cool atoms to then excite them to the Rydberg state. This makes it possible to carry out experiments to study the interaction between atoms and light.

The NQO project focuses on different atoms such as Rubidium and Ytterbium. In the Ytterbium Rydberg group (YQO), ultra-cold Ytterbium is used to study systems of strongly interacting Rydberg polaritons and to measure the binding energies of ultra-long range Rydberg molecules of Ytterbium. For that, lasers are used as probe and control beams [3].

To further optimize the experimental setup, two new high power diode lasers (DL pro HP by TOPTICA Photonics) were bought. A requirement for the implementation of these diode lasers is, that those lasers have a narrow linewidth and a well defined controllable frequency.

Depending on the application, the frequency of the laser can be stabilized to a reference frequency given by an atomic transition or by another laser. For the future use of the lasers, they need to be frequency stabilized to another laser, which is the aim of this thesis.

In this thesis project, one of the lasers was frequency stabilized to the other free-running laser. The first step of this process was to install the lasers and characterize aspects like the beam profile and the laser thresholds. For the frequency stabilization itself, I first optical overlapped both beams. In the next step, I built a setup similar to the one implemented in the paper *A versatile digital GHz phase lock for external cavity diode lasers* by Jürgen Appel et al. [4] to generate an error signal depending on the relative frequency between the beat note frequency of the overlapped beams and a fixed reference

frequency. For the setup of the error generation, I used an ADF4007 evaluation board built by Analog Devices [5]. With the generated error signal, I setup and optimized a dual-feedback loop. Finally, I was able to verify the operation of the feedback loop by measuring the linewidth of the beat note and the duration of the slave laser stabilization.

Diode lasers in Littrow-configuration

The choice of laser depends on the specific requirements of each application, as different types of lasers offer unique physical and operational parameters. In general, lasers allow the use of nearly monochromatic light which is important for experiments that need a light source with a distinct wavelength. However, the monochromaticity of the laser frequency is limited due to small fluctuations on different time scales. These fluctuations are caused by effects like changes in the voltage applied to the piezo or the laser current, as well as mechanical effects of thermal influences, electronic noise, acoustic interference, and many other factors. As a result, lasers do not have the desired long-term wavelength stability and narrow line width without further stabilization. [1]

The operating principle of lasers is based on stimulated emission, in which an active medium is energetically stimulated and as a result releases energy in form of photons. The most common types of lasers based on high density active media are solid-state, dye and semiconductor lasers. [1] The lasers used in this bachelor thesis are external-cavity diode lasers (ECDL) in the Littrow configuration. This type of lasers use a diode with a pn-junction as the active medium.

The operating principle of diodes is based on semiconductor physics, where electrons are lifted from the so-called valence band into the conduction band by applying an external current. Light emission occurs, when electrons of the conduction band fall back into the valence band recombining with a so-called hole. In laser diodes, the excitation of the electrons is achieved by a current flowing in the forward direction of the junction. Thus, diode lasers allow direct transformation of electrical current into coherent light, which is why they are one of the most used laser types. A detailed description can be found in *9.4.1. Principle of Semiconductor Laser Operation*. [6]

In the Littrow configuration, see figure 2.1, the laser diode and the collimator are followed by a grating. The grating is used to reflect the 1st order of the laser beam directly back into the light source. This order of the beam represents 5-15 % of the beam power. The 0th order of the laser beam can then be used for applications. Reflecting a part of the light directly back into the light source causes a frequency-selective feedback and a corresponding modulation of the gain profile. Thus, turning the grating allows the laser to be tuned to almost every wavelength within its gain profile without modifying its facet reflectivities. [1]
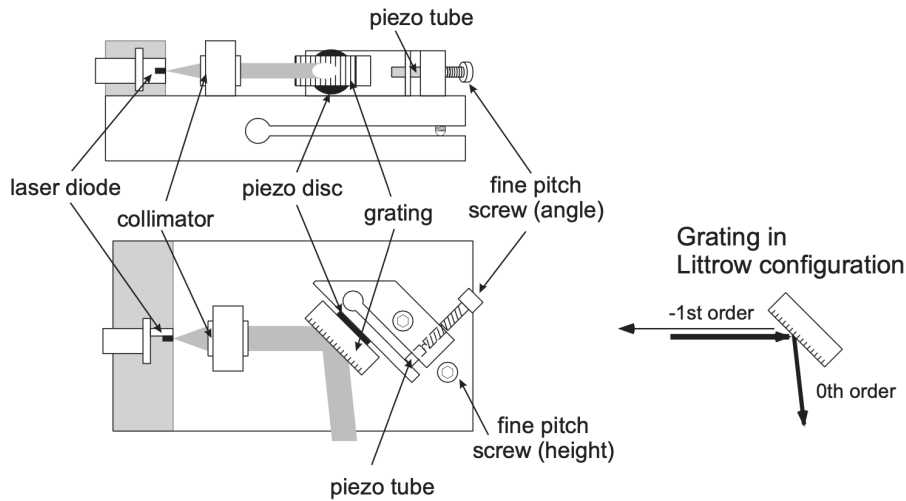
Figure 2.1: Schematic layout of a laser in Littrow configuration. The 1st order is reflected into the laser diode and the 0th order is used for applications. [1]

2.1 Frequency tuning

The frequency of the emitted laser beam is determined by the hardware setup of the laser as well as settings of the laser, such as the diode current and the laser temperature.

The fundamental range of the wavelength is determined by the laser diode: Depending on the band gap of the semiconductor materials of the diode, the frequency of the laser varies; materials with a higher band gap emit light at a higher frequencies.

Additionally, one can directly change the injection current of the diode. On the one hand, this changes, the charge carrier density and thus the refractive index. On the other hand, it changes the diode temperature and thus the junction temperature due to Joule heating. A change in temperature has a direct impact on the value of the frequency. This is due to the fact that both the optical path length of the cavity and the wavelength dependence of the gain curve are temperature dependent. It is also possible to separately change the temperature of the laser diode itself.

Moreover, the length of the optical cavity modifies the resulting frequency as it not only has an impact on the wavelength but also on the mode-hop free tuning range. However, the length of the optical cavity is determined by the manufacturer and therefore not easily changeable.

Due to the effect of optical feedback through the grating, the position of the grating can change the resulting frequency. The position of the grating can be changed manually and electronically. Since, the rough grating position is set by the manufacturer, only its angle can be adjusted by turning the fine pitch screw as shown in 2.1. With the grating being positioned on a piezo actuator, the grating position can be fine-tuned by changing the voltage applied to the piezo actuator.

Since both the temperature and the current affect the frequency by not one, but two mechanisms each with different shifting parameters, laser frequency tuning needs to be performed iteratively. Thus, to tune the laser beam to a specific frequency with minimal mode hopping, the laser needs to be not only roughly tuned to the desired frequency by changing the current and voltage applied to the piezo, but also the current, voltage, temperature and grating angle need to be changed iteratively until the laser runs in single mode at the desired frequency. [7] [8]

2.2 Determining the beam profile

The resulting beam emitted by the laser is a collimated gaussian beam, which means that the light is axially symmetric and stays nearly constant over large distances. The intensity profile perpendicular to the propagation of the beam can be described as:

$$I(\rho, z) = \frac{c\epsilon_0}{2} \cdot EE^* = \frac{c\epsilon_0}{2} |A_0|^2 \left(\frac{w_0}{w(z)}\right)^2 e^{-2[\rho/w(z)]^2}. \qquad [1] \tag{2.1}$$

The axial peak value can be described as:

$$I(0, z) = \frac{c\epsilon_0}{2} |A_0|^2 \left(\frac{w_0}{w(z)}\right)^2. \qquad [1] \tag{2.2}$$

As shown in figure 2.2, the beam inside the cavity is focused due to the limitation caused by the mirrors, which forms a minimal beam waist w_0. The exact position of the beam waist depends on the form of the cavity: For a confocal cavity, the position of w_0 is in the middle of the cavity. With the wavelength λ, the beam width at any position in the cavity can be described with:

$$w(z) = w_0 \left[1 + \left(\frac{\lambda z}{\pi w_0^2}\right)^2\right]^{1/2}. \qquad [9] \tag{2.3}$$

In figure 2.2, the divergence of the beam is described as Θ. The distance in which the beam radius increases by a factor of $\sqrt{2}$ and the cross sectional area by a factor of 2 is called the Rayleigh range. This distance z_R, is defined by:

$$z_R = \frac{\pi w_0^2}{\lambda}. \qquad [9] \tag{2.4}$$

The beam outside the cavity is an extension of the beam shown in figure 2.2. The divergence of that beam can be understood as a continuation of the divergence of the in figure 2.2 shown beam. The intensity of the general laser beam follows a Gaussian distribution. This means that the intensity of the beam (along the x and y propagation) is the highest at the center of the beam.

In order to test both newly installed lasers, I measured the beam profiles of the master and the slave lasers with a so-called beam profile camera directly behind the lasers and in a distance of approximately (37.0 ± 0.1) cm. The beam profile camera illustrates the beam profile of a laser beam and calculates beam parameters such as the beam diameter along the x- and y-axis by fitting a gaussian curve along
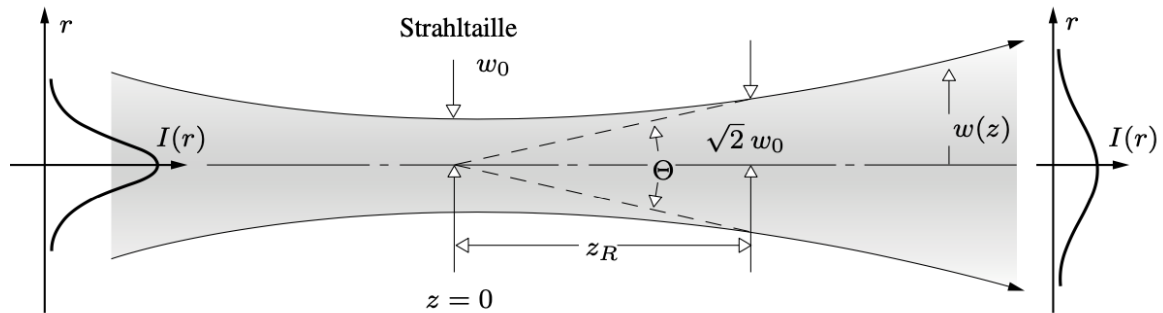
Figure 2.2: Broadening of a Gaussian beam. Shown is a Gaussian beam between two concave mirrors with the distance of $d = 2z_r$. If one of the mirrors is coated with silver, the beam passes with a divergence of θ.

both axes. In figures 2.3 and 2.4, the resulting beam profiles can be seen. The profiles of both lasers show that the beam shape changes over distance. This can be seen by the reduction of the diameters of both lasers along the distance: The diameters of the beam leaving the slave laser were 1.763 mm along the x-axis and 0.741 mm along the y-axis. However, after a propagation of approximately 37 cm, the diameters were 1.684 mm along the x-axis and 0.815 mm along the y-axis. The beam diameters of the master laser were first 1.566 mm along the x-axis and 0.724 mm along the y-axis. After approximately 37 cm, they were 1.534 mm along the x-axis and 0.827 mm along the y-axis. This change in diameters can be explained by the loss of intensity of the beam due to air propagation: With increasing distance, the beam profile looses intensity and thus the intensity of the edges of the beam profiles lessen as well, resulting in a decreased diameter.

Apart from the intensity loss of the beams, one can see that the profiles of the beams are elliptical. This elliptical shape is caused by the rectangular shape of the diode. [8] In order to make the beam shape nearly radially symmetric, one can use anamorphic prisms which magnify the elliptical beam in one dimension. [10] However, in the following setup, this adjustment was not necessary as the shapes of the lasers are sufficiently similar enough for the following optical beatnote.
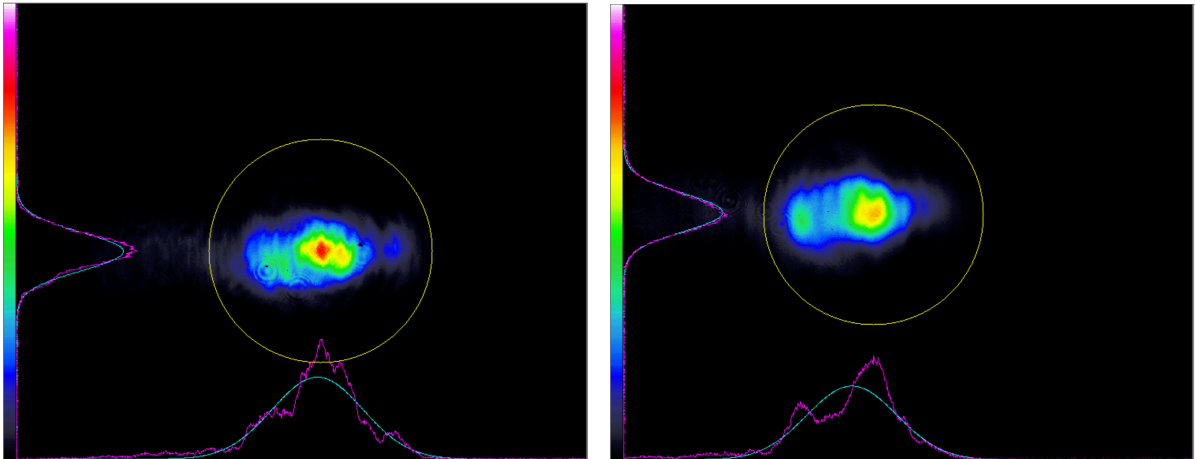
(a) Slave laser. Beam profile measured behind the laser. Measured diameters: 1.763 mm along the x-axis and 0.741 mm along the y-axis

(b) Slave laser. Beam profile measured in a distance of approximately 37 cm. Measured diameters: 1.684 mm along the x-axis and 0.815 mm along the y-axis

Figure 2.3: Beam profiles of the slave laser over course of its propagation. Shown are the beam profiles of the laser in x- and y-direction fitted with a Gaussian curve and additionally the intensity of the beam. The power of the laser was $P = 455\,\mu$W
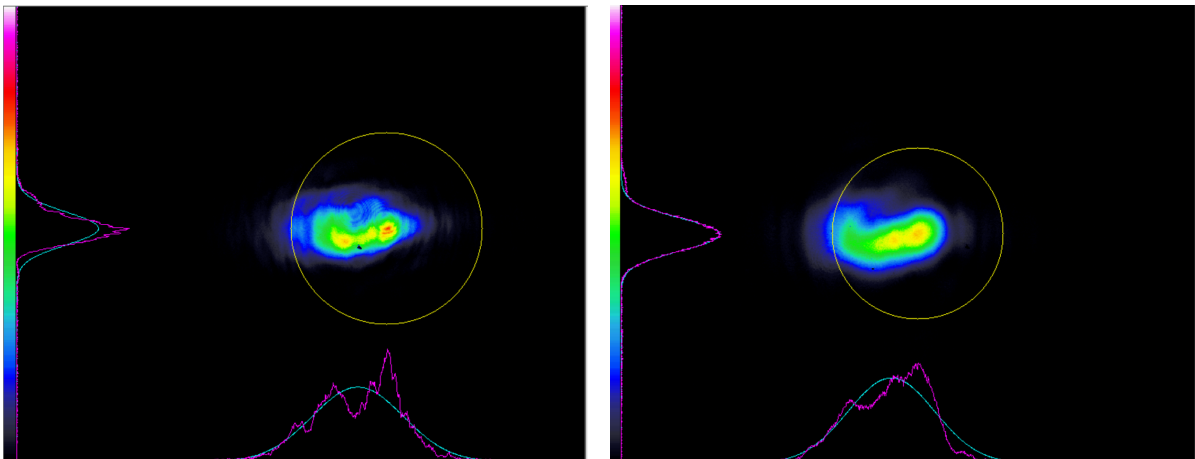
(a) Master laser. Beam profile measured behind the laser. Measured diameters: 1.566 mm along the x-axis and 0.724 mm along the y-axis

(b) Master laser. Beam profile measured in a distance of approximately 37 cm. Measured diameters: 1.534 mm along the x-axis and 0.827 mm along the y-axis.

Figure 2.4: Beam profiles of the master laser over course of its propagation. Shown are the beam profiles of the laser in x- and y-direction fitted with a Gaussian curve and additionally the intensity of the beam. The power of the laser was $P = 400\,\mu$W.

2.3 Determining the current threshold

The dependence of the emitted laser power on the current applied to the diode can be seen in figure 2.5. It depicts the laser power measured with a power meter for different currents applied to the laser diode.

By calculating a linear fit for these data points, the lasing threshold of both lasers can be determined. As shown in the figures, both measured thresholds match the specified threshold given by the manufacturer Toptica. The current threshold is determined by the diode of the laser: Depending on the band gap of the semiconductor, the threshold can be higher or lower. However, the threshold not only depends on the band gap of the diode but also on e.g the temperature. A higher temperature, for example, can lead to a lower threshold. In *Principles of Lasers* by Orazio Svelto, these correlations are explored further. [6]
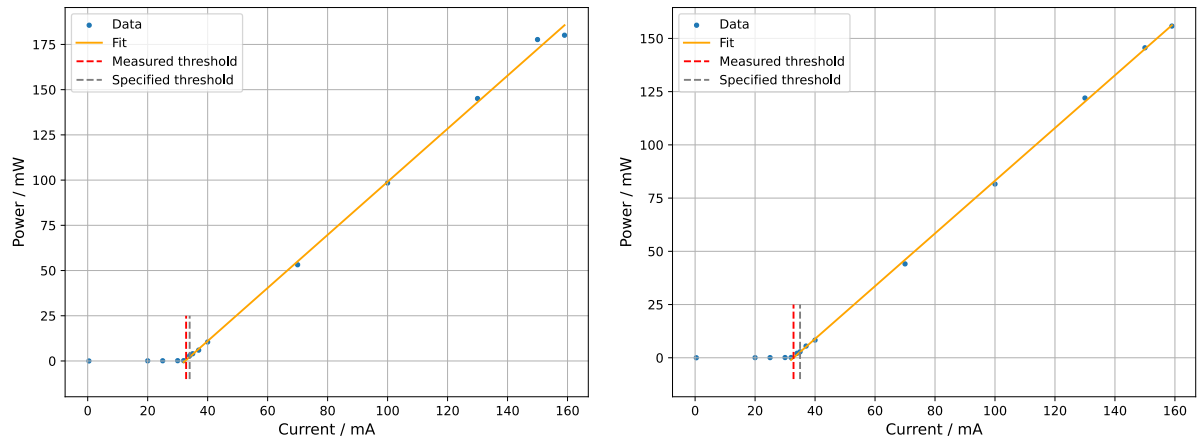
(a) Measurement of master laser threshold with estimated threshold of: (32.5 ± 1.3) mA.

(b) Measurement of slave laser threshold with estimated threshold of: (32.5 ± 1.3) mA.

Figure 2.5: Measurement of laser threshold.

The optical beat note

To stabilize the frequency of a laser, it is essential that the beams of the slave and master lasers overlap. This causes both lasers to interfere, which is noticeable in the overall intensity $I(r)$. This overall intensity consists of the intensities $I_1(r)$ and $I_2(r)$ of each of the lasers. With $g_{12}(r, \tau)$ being the normalized correlation function, the overall intensity $I(r)$ can be calculated for coherent and incoherent superposition by:

$$\langle I(r) \rangle = \langle I_1(r) \rangle + \langle I_2(r) \rangle + 2\sqrt{\langle I_1(r) \rangle \langle I_2(r) \rangle} \, \text{Re}(\{g_{12}(r, \tau)\}) \tag{3.1}$$

$$\text{with:} \quad g_{12}(r, \tau) = \frac{(c\epsilon_0/2)\langle E_1(r, \tau)E_2^*(r, 0)\rangle}{\langle I_1(r)\rangle\langle I_2(r)\rangle}. \qquad [1] \tag{3.2}$$

The coherence of both laser beams can be quantitative measured by the visibility (or contrast) V. The overlap between the two lasers can thus be quantified by the highest I_+ and lowest I_- value of the superposition intensity.

$$V = \frac{I_+ - I_-}{I_+ + I_-}. \qquad [1] \tag{3.3}$$

The visibility can take values between 0 and 1, where values close to 0 mean a low coherence and values close to 1 a high coherence.

3.1 Optical Setup

For this project, the overlap of the slave and the master laser was realized as shown in the optical setup in figure 3.1. Both laser beams are first polarized by the half wave plate. Afterwards, the polarizing beamsplitter (PBS) divides the beams of the lasers; the horizontal polarized part is transmitted while the vertical polarized part is reflected. Then, a beam sampler reflects nearly 10 % of the vertical part of the beam which is then coupled into a fiber leading to a wavemeter monitoring the wavelength of the beams.

To further reduce the power of the master laser beam and thus preventing damage to the wave meter, an ND filter is placed between the beam sampler and the fiber going to the wave meter. The part of the
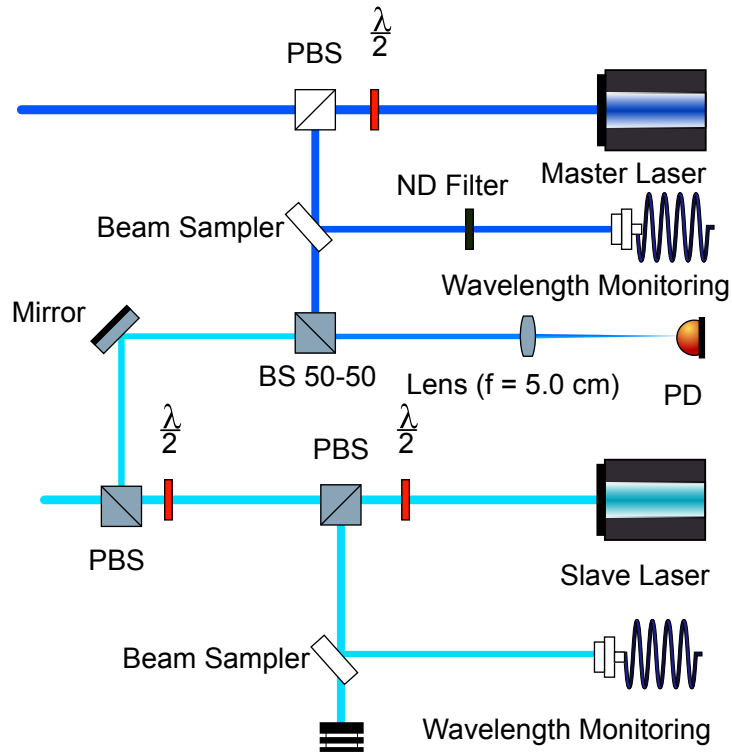
Figure 3.1: Optical setup used to overlap the beams of the master and the slave laser. In order to monitor the wavelength of both laser beams, the part of the laser beams reflected by the beam sampler is coupled into a fiber that is connected to a wavemeter. For the purpose of matching the polarization of both beams polarizing beamsplitters (PBS) are used.

master laser that is transmitted by the beam sampler is then divided by a 50:50 beamsplitter: Half of the beam is reflected and the other half is transmitted. The reflected part of the beam is focused onto a photodiode by a lens with a focal length of 5 cm.

In order to overlap slave and master laser with the same polarization direction, the transmitted slave laser beam is first rotated by a half wave plate and then reflected by another PBS. Afterwards, it is reflected by a mirror and then transmitted by the 50:50 beamsplitter similar to the master laser beam. Finally, the overlapped focused beam is translated into a current by the photodiode.

3.2 Overlap improvement

It can be sufficient to monitor the coupling of both beams onto the photodiode with an oscilloscope and then observe the resulting beatnote with a spectrum analyzer. In this case, however, it was necessary to further improve the coupling of both beams onto the photodiode and thus the resulting beatnote. The following sections describe the steps I took.

3.2.1 Improving the beam size

Firstly, I ensured that the beam diameter of the focused beam matched the size of the photodiode by monitoring the beam profile with the beam profile camera as shown in figure 3.2. Thus, I was able to test the position of the lens. With an estimated beam diameter of 0.179 mm in x-direction and 0.124 mm in y-direction for the slave laser (fig. 3.2(b)) and 0.134 mm in x-direction and 0.084 mm in y-direction for the master laser (fig. 3.2(a)) both beam sizes fit the size of the photodiode which has an effective sensitive area of 0.2 mm x 0.2 mm. [11]
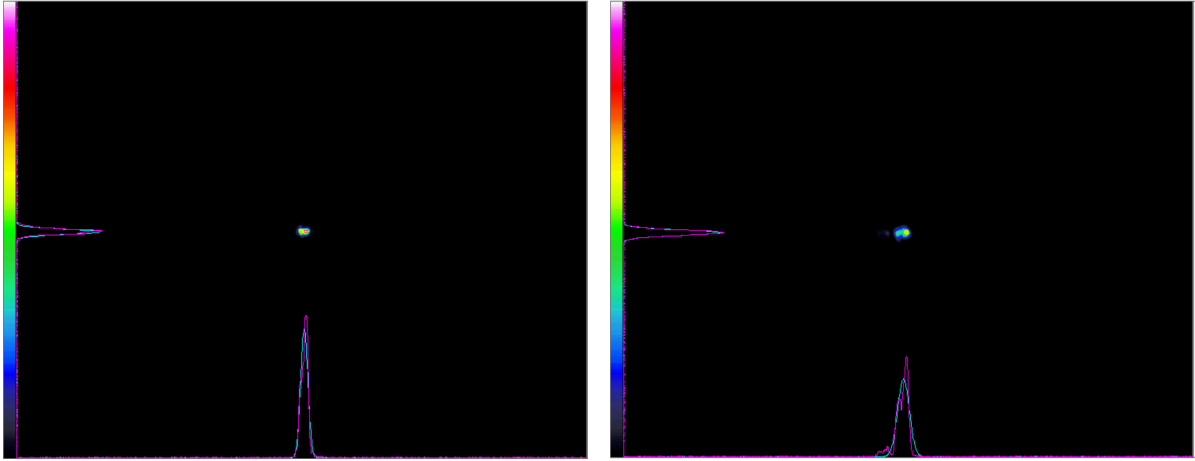
(a) Focused Beam Profile Master Laser. Beam diameter: 0.179 mm in x-direction and 0.124 mm in y-direction.

(b) Focused Beam Profile Slave Laser. Beam diameters: 0.134 mm in x-direction and 0.084 mm in y-direction.

Figure 3.2: Measurement of beams profiles focused by a lens with focal length of 5 cm

3.2.2 Improving the visibility

One can further improve the overlap by improving the visibility of the overlapped beam. For this, I used a PDA10A2 photodiode connected to an oscilloscope to measure the voltage of the photodiode over time. The resulting voltage amplitude (see fig. 3.3) is in direct correlation to the interference of the overlapped beams. In order to calculate the visibility, I fitted the in equation 3.4 cosine function to the data:

$$U(t) = A\cos(\omega_{beat} \cdot t) + b \tag{3.4}$$

Using this fit, the visibility V is calculated accordingly to equation 3.3. By repositioning the mirror and the second PBS of the slave laser, I was able to improve the visibility from $V = (0.543 \pm 0.005)$ to $V = (0.609 \pm 0.004)$ as shown in figure 3.3.

From equation 3.4, one can calculate the beat frequency according to equation 3.5.

$$f_{beat} = \omega_{beat}/2\pi \tag{3.5}$$

The beat frequency of the beat note before realigning the slave laser is: (71.2566 ± 0.0005) MHz and after the realignment: (65.8803 ± 0.0004) MHz. The change of the beat frequency can not only be

(a) Before adjustments: $V = (0.543 \pm 0.005)$.

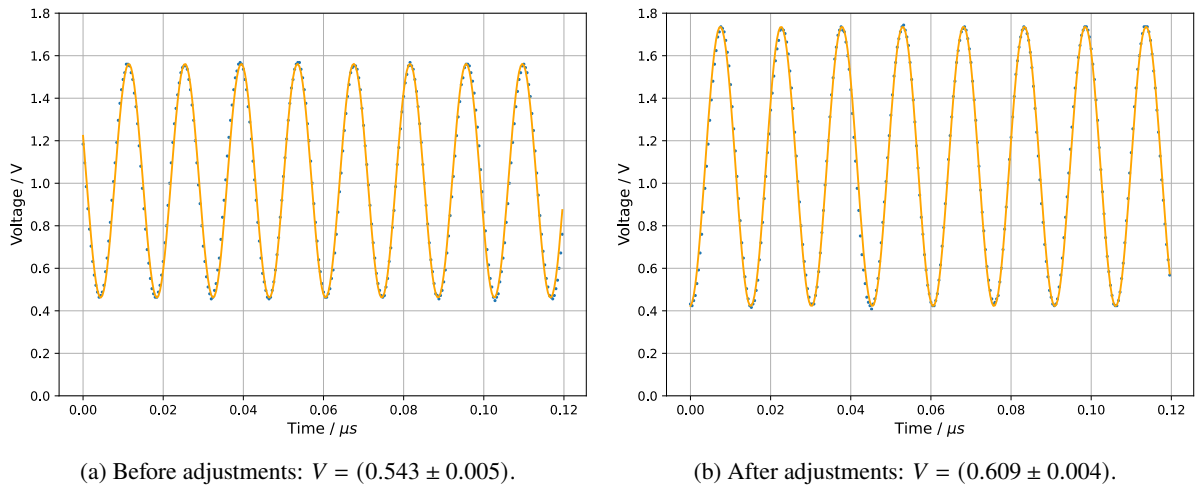(b) After adjustments: $V = (0.609 \pm 0.004)$.

Figure 3.3: Measurement of contrast for improving overlap of both lasers.

explained by the improved alignment of the laser but also by a change of the frequencies of both lasers. The lasers were not stabilized over the course of the measurement and thus the frequencies could have shifted resulting in a shift of the beat frequency.

3.3 The beat note signal

Lastly, I was able to observe the beat signal on a spectrum analzyer using a fast photodetector (Hamamatsu G4176-03 [11]). In order to use the photodetector, a bias-voltage needs to be provided (e.g. by a bias-tee). The observed signal is depicted in figure 3.4. The graph shows that the difference of the frequencies of both lasers was approximately 1 GHz. Moreover, one can see that in the shown frequency range, both lasers are running mostly mode-hop free. This will be further analyzed in chapter 5.
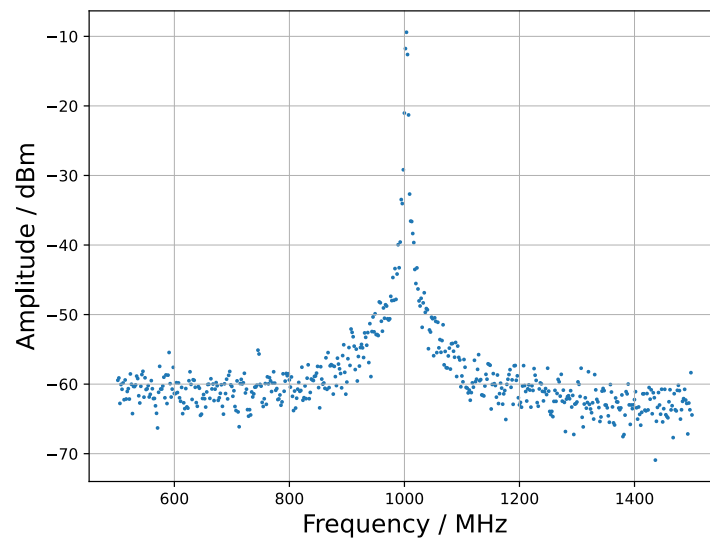
Figure 3.4: Measurement of beat note without frequency stabilization. The beat note is amplified by 42 dBm as further explained in chapter 4.

Generating an Error Signal

To build the feedback loop needed for the stabilization of the slave laser, it is essential to maintain a fixed value of the relative phase between the master laser and the slave laser. This fixed value f_{beat} is the beat frequency as described in section 3.2.2. An optical phase-locked-loop (OPLL) will be realized to maintain the beat frequency automatically on that fixed value through a feedback loop. In order to generate an error signal for said feedback loop, the signal of the optical beat note realized in chapter 3 will be compared to a reference frequency.

4.1 Setup

To generate an error signal based on the signal of the beat note and a tuneable reference frequency, I built a setup similar to the one implemented in the paper by Jürgen Appel et al. [4]. The main element of the setup is the ADF4007 evaluation board by Analog Devices which is a high frequency divider/PLL synthesizer. [12]

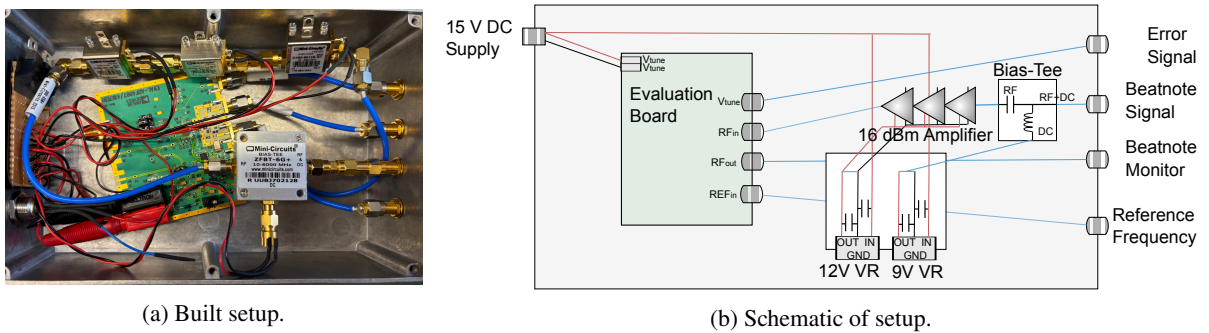
(a) Built setup.

(b) Schematic of setup.

Figure 4.1: Setup to generate an error signal.

As shown in figure 4.1, the setup consists of a bias-tee that is used to provide a bias-voltage for the Hamamatsu photodiode of the optical setup, three amplifiers (ZX60-6013E+), and an evaluation board. In order to power the bias-tee and the amplifiers, I connected the amplifiers to the output of a 12 V

14

voltage regulator and the bias-tee to the output of a 9 V voltage regulator.

With this setup, the incoming beat note signal is amplified by 48 dBm. The incoming signal of the beat note can be observed with a spectrum analyzer connected to a monitor output. Note here, that the signal is decreased by −6 dBm [12] due to the setup of the evaluation board. The amplification of the signal is necessary so that the signal will be high enough to be processed by the evaluation board. First, the beat note signal is converted from sine waves into digital pulse trains by counters implemented in the board. Due to the setup of the board, the resulting beat note is divided by 16 and compared to the reference frequency, which is divided by 2. [12] The frequency and phase of both signals are then compared by a dual flip-flop circuit. Depending on the value of the frequency difference (the beat frequency), an error signal with a specific voltage is generated: If the beat frequency is higher than 0, the voltage of the error signal is near the maximum, if the beat frequency is zero, it gives out half of its maximum and if the beat frequency is lower than zero, it gives out a voltage near 0 V.

The maximum voltage of the resulting error signal can be set by a jumper to either 3 V or 5 V. [12] That changes not only the maximum output voltage, but also the rise time of the signal during a change from a negative difference of both laser frequencies to a positive difference (see fig. 4.2). To ensure that the stabilizing setup performs optimally, I compared the rise time of the error signals. A lower rise time ensures a faster reaction of the feedback-loop. Figure 4.2 shows that the rise time for 3 V is (0.0858 ± 0.0001) ms and for 5 V is (0.1326 ± 0.0001) ms. Since the rise time of the error signal with the jumper set to 3 V is shorter than with the 5 V setting, I used the 3 V setting for the feedback loop. The sign of the voltage depends on the sign of the phase of the beat note and thus on the sign of the beat frequency. [12]
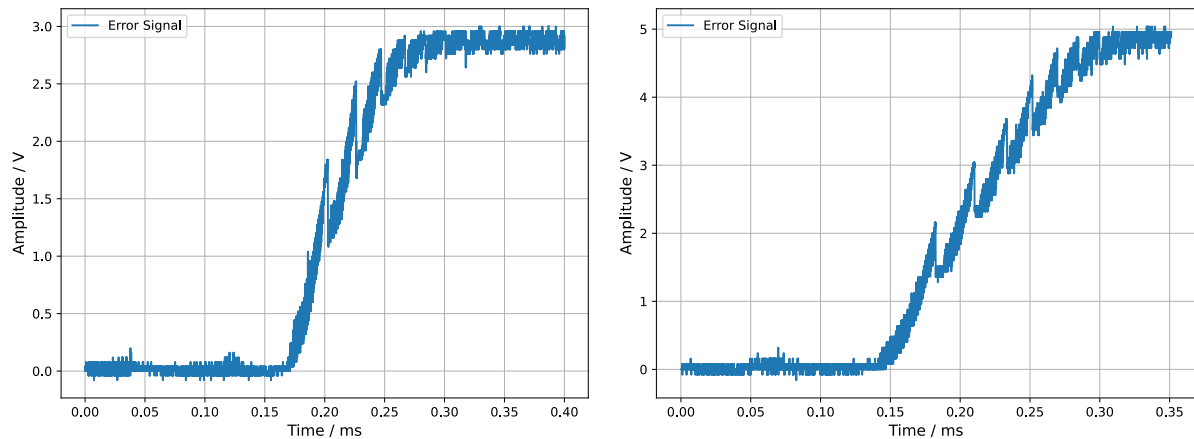
(a) Error signal while scanning laser over reference frequency with jumper set to 3 V with estimated rise time of (0.0858 ± 0.0001) ms.

(b) Error signal while scanning laser over reference frequency with jumper set to 5 V with estimated rise time of (0.1326 ± 0.0001) ms.

Figure 4.2: Comparison of rise time of error signal.

4.2 Limitations and outlook

The setup used to generate the error signal (see fig. 4.1) has certain limitations, one of which is the maximum bandwdith of 7.5 GHz [12] of the evalutation board. Another limitation is caused by the RF amplifiers. Here, the gain of the amplifiers decreases for higher frequencies (see [13]). Furthermore, the insertion loss of the RF cables increases for higher frequencies. These limitations cause a decrease of the beat note amplitude for higher frequencies as shown in figure 4.3.
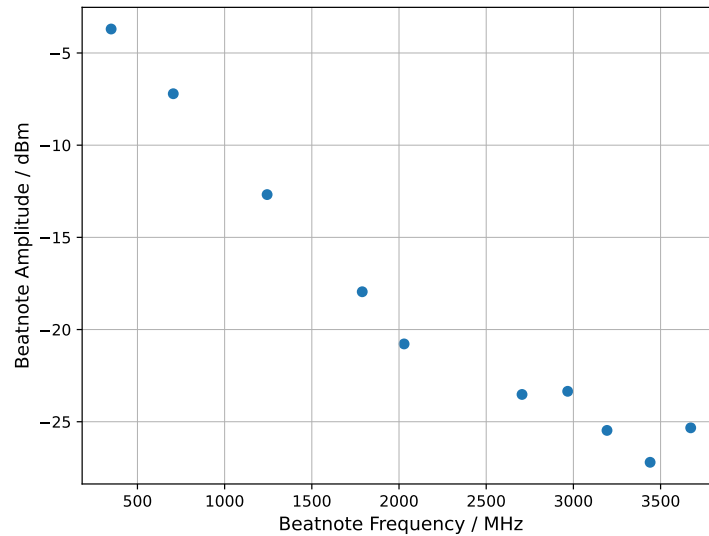

Figure 4.3: Beat note amplitude measured with a spectrum analyzer for different beat note frequencies.

In order to improve the range of the beat note frequencies, one can use gain equalizers. These gain equalizers are frequency dependent attenuators that are able to compensate the inhomogeneous gain of the amplifier. Thus, the combination of the amplifiers and the gain equalizer could lead to a slower decrease of the beat note amplitude for higher frequencies 4.3.

Creating a feedback loop

The error signal described in chapter 4 can be used to stabilize the slave laser with the master laser. For that, a feedback loop consisting of a current and a piezo feedback loop is built using a proportional-integral-derivative (PID) regulator. The PID levels the error signal generated by the evaluation board (fig. 4.1) and provides a feedback to the controller of the slave laser.

5.1 The PID regulator

As suggested by the name, PID controllers have three parts: A proportional K_P, an integral K_I and a derivative K_D gain. The overall gain $G(s)$ of the controller is described as:

$$G(s) = K_P + K_I \frac{1}{s} + K_D\, s \qquad [14] \tag{5.1}$$

In the feedback loop, each of the gains have a different functionality: The proportional term provides an overall control action proportional to the error signal through the all-pass gain factor. The integral term reduces steady-state errors through low-frequency compensation by an integrator. The derivative term improves transient response through high-frequency compensation by a differentiator. Together, all of these parameters help to stabilize the feedback loop to a steady value. [14]

5.2 Realization of the feedback loop

In this setup, the PID regulator is implemented in the FALC pro by Toptica Photonics. The FALC consists of a PI^3D^2 regulator and a PI regulator. [15] In combination with the generated error signal and the controller of the lasers (DLC), a feedback loop can be realized to frequency stabilize the slave laser.

Since the instantaneous bandwidth of typical ECDLs has a range of up to a few hundred kilohertz, the loop needs to be fast enough to correct for this noise. Additionally, the loop needs to be able to correct low-frequency noise and drifts stemming from mechanical vibrations. In order to achieve both noise corrections, a dual feedback was implemented as shown in figure 5.1.
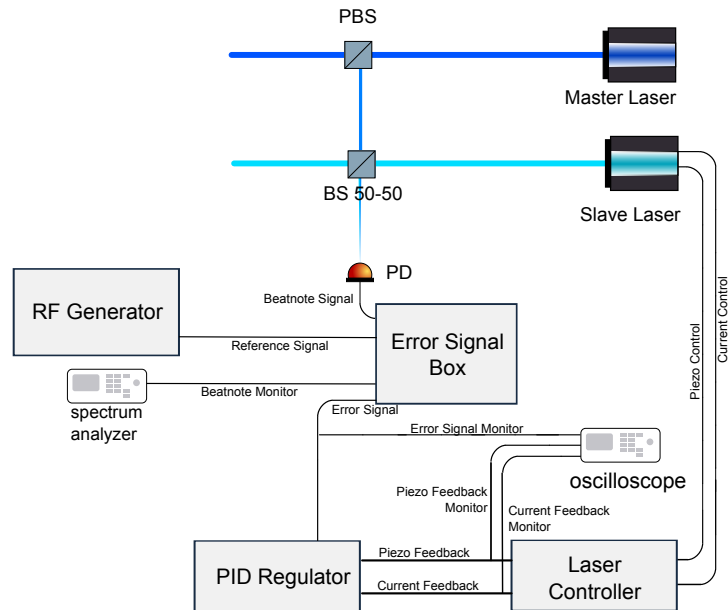
17

Figure 5.1: Setup of Feedback Loop

As shown in figure 5.1, the laser beams of the slave and the master laser are first optically overlapped as explained in chapter 3. The signal of the beat note is then processed by a fast photodiode and compared with a reference frequency by the evaluation board (error signal box). The reference frequency is generated by a modifiable RF generator (Arduino DDS board). Depending on the desired frequency difference between the lasers, the RF generator can be tuned accordingly. The generated error signal is then given to the PID (FALC pro). The PID generates the feedback signals for the controller of the slave laser, which closes the feedback loop.

Due to the fact that the frequency tuning mechanisms described in chapter 2 operate on different time scales, dual feedback can be implemented by using different electrical tuning mechanisms for different feedbacks: Since current injection modulation is fast (up to a few MHz), but frequency corrections are limited by mode hops, current modulation is used for fast feedback of the dual-feedback loop. The modulation of the external cavity length, which is done by applying a voltage to the piezo, is used for the slow feedback. This is because the bandwidth of the piezo modulation is limited by mechanical resonances to a few kHz, while it allows significant correction of the laser frequency. [4]

5.3 Optimization of the feedback loop

To ensure the function of the feedback loop, the parameter of both the current and the piezo feedback loop needs to be optimized. In order to do that, I first optimized the current feedback, which operates on faster time changes and afterwards optimized the piezo feedback.

5.3.1 Current feedback

In order to optimize the current feedback loop, I started by optimizing the gain of the PID controller. For that, I changed the frequency of the master laser so that the resulting beat note oscillates around the reference frequency as shown in figure 5.2. While monitoring the resulting error signal of the PID (current feedback), I adjusted the offset, so that the error signal of the current feedback oscillates around zero. The optimized input offset is set to 1.43 V.
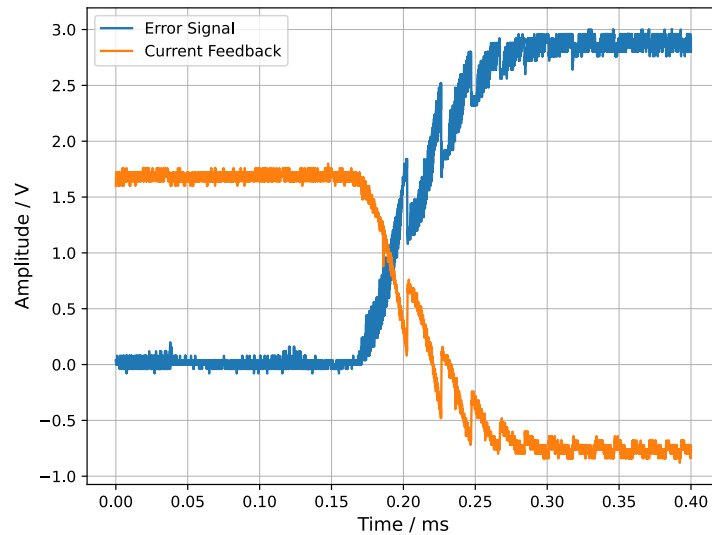

Figure 5.2: Error signal and current feedback.

Afterwards, I improved the individual gains of the PID. As previously mentioned, the FALC consists of a PI^3D^2 regulator, meaning that there are multiple integral (I) and derivative (D) gains that can be modified. First, I corrected values for I_1 and the proportional gain (P) iteratively while monitoring the beat note on the spectrum analyzer. Then, I adjusted the value for I_2 while changing the values for I_1 and the gain as well. The optimized parameters are: $I_1 = 7.0\,\mathrm{MHz}$ and $I_2 = 5.0\,\mathrm{kHz}$. By adjusting these parameters, I made sure that the beat note amplitude locks to the reference frequency and the error signal of the FALC goes towards zero. Then I improved the bandwidth of the control loop by adjusting D_2 while ensuring that the servo bumps are as low and far away from the beat note maximum as possible. The adjusted parameter value is: $D_2 = 420\,\mathrm{kHz}$. Then I adjusted D_1 as shown in figure 5.3. By adjusting this parameter I ensured that the servo bumps are as far away as possible from the beat note maximum while ensuring that the amplitude of the peak does not decrease too much. This adjusted value was found at $D_1 = 1.5\,\mathrm{MHz}$.

5.3.2 Piezo feedback

The optimization of the piezo feedback works similar to the optimization of the current feedback: First I adjusted the offset while looking at the error signal of the FALC and adjusted the offset so that the error signal oscillates around zero again. The resulting value for the offset is: $-0.91\,\mathrm{mV}$. Then I used small disturbances such as closing the lab door or pressing on the optical table to disturb the laser and thus the
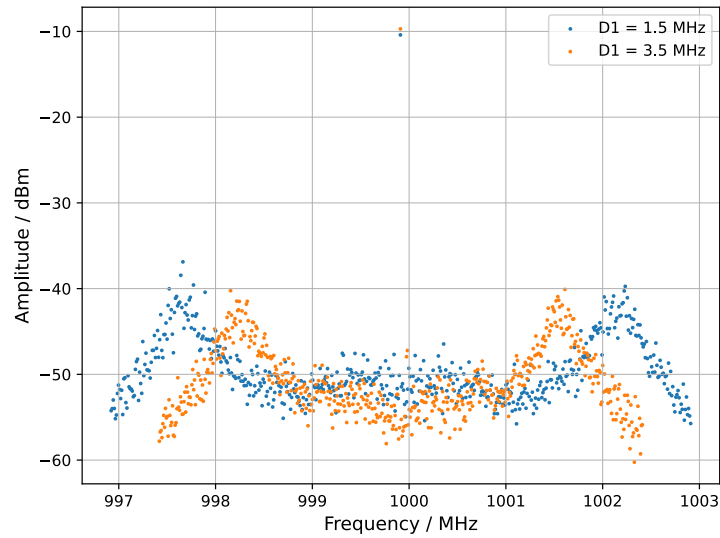
Figure 5.3: Comparison of position of servo bumps for different values of D_1.

error signal of the FALC. As shown in figure 5.4 the lock was then able to correct for a small disturbance. In this figure, one can see that only the current feedback tries to correct the frequency instability of the laser while the piezo feedback stays nearly constant and does not correct much. By separating the time scale that both feedbacks are acting on, one can prevent that both feedback loops try to correct each other. With this optimization technique, I was able to improve the PI parameters of the FALC used for the piezo feedback.
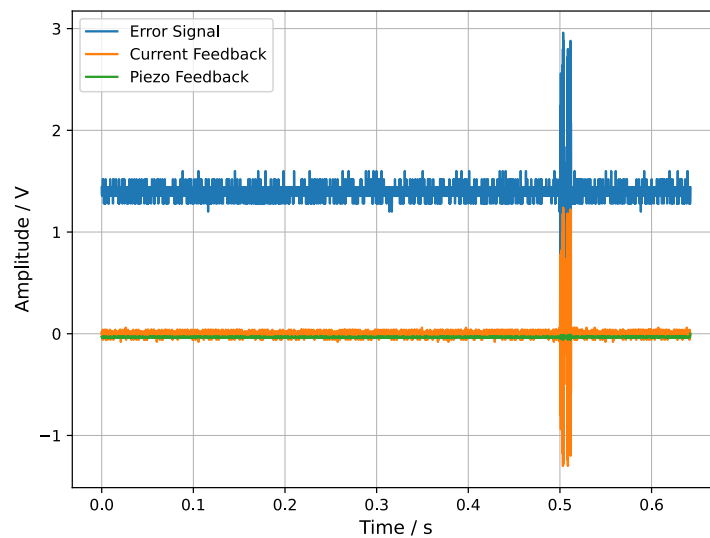

Figure 5.4: Error signal (blue), current feedback (orange) and piezo feedback (green) measured with and oscilloscope while disturbing the laser.

5.4 Verifying the stabilization

In order to verify the stabilization, I measured the beat note signal and calculated the linewdith of the signal by fitting an approximation of the Voigt curve to the data. There are several different methods to calculate the linewidth: With a Lorentzian, Gaussian or Voigt curve (or an approximation of the Voigt curve). [16] [17] Because of the form of my data points, I used a Voigt curve which is a combination of a Gaussian $f_{\text{Gaussian}}(x)$ and a Lorentzian $f_{\text{Lorentzian}}(x)$ curve:

$$f_{\text{Voigt}} \approx (1 - \mu)\, f_{\text{Gaussian}}(x) + \mu\, f_{\text{Lorentzian}}(x) \qquad [16]. \tag{5.2}$$
$$\tag{5.3}$$

In the Gaussian function, A is the amplitude, σ the variance and μ the expected value:

$$f_{\text{Gaussian}}(x) = \frac{A}{\sigma\sqrt{2\pi}} \cdot e^{-\frac{(x-\mu)^2}{2\sigma^2}}. \tag{5.4}$$

In the Lorentzian function, x_0 is the location parameter of the mean and γ is half of the full width at half maximum FWHM.

$$f_{\text{Lorentzian}}(x) = \frac{I}{\pi}\left[\frac{\gamma^2}{(x - x_0)^2 + \gamma^2}\right]. \tag{5.5}$$

For the Voigt-fit, I added a constant offset to the fit-function, depending on the data. The resulting linewidths (in this case FWHM [16]) can then be calculated by the parameters of the Voigt-fit as follows:

$$\text{FWHM}_{\text{gaussian}} = 2\sqrt{2\log 2}\, c \approx 2.35482\, \sigma \tag{5.6}$$
$$\text{FWHM}_{\text{lorentzian}} = 2 \cdot \gamma. \tag{5.7}$$

In order to show that the measured linewidth is impacted by the resolution of the spectrum analyzer, I measured the signal of the beat note three times: Once while it is free running and then twice while it is stabilized with two different resolution bandwiths (RBW) of the spectrum analyzer, as shown in figures 5.5 and 5.6.

The linewdiths calculated according to equations 5.4 and 5.5 of each measurement are depicted in table 5.1. Since the measurements were limited by the resolution of the spectrum analyzer, the RBW was included in the table. As one can see, stabilizing the slave laser decreases the linewidth of the beat note signal, verifying that the laser stabilization was successful.

Table 5.1: Measured FWHM

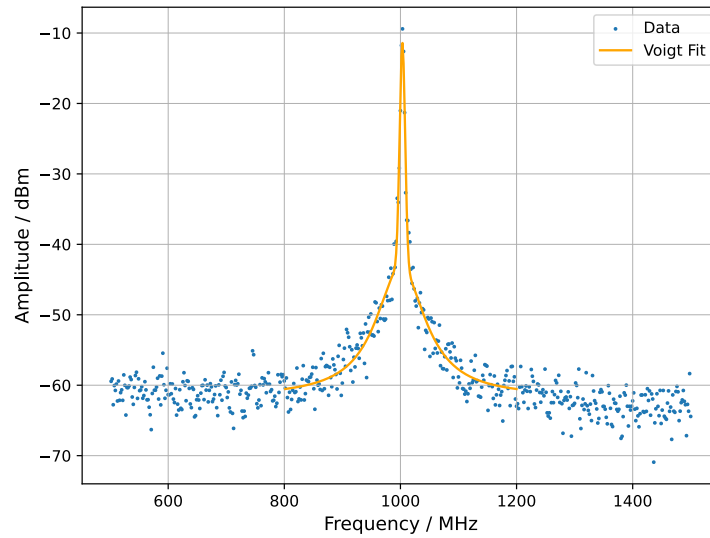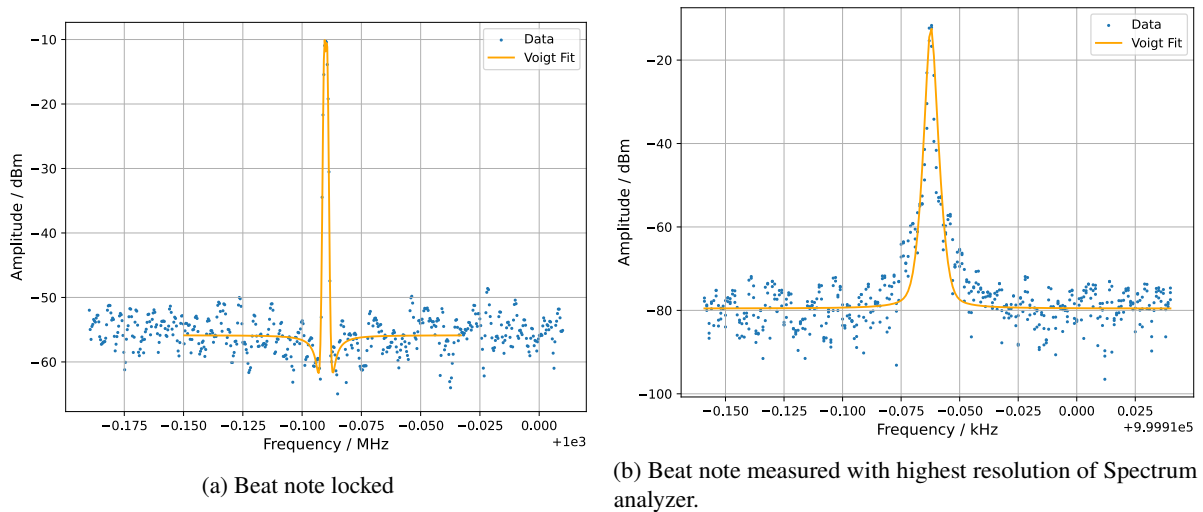| Figure	RBW	Gaussian	Lorentzian
Unstabilized beat note (fig. 5.5)	3 MHz	(7.8 ± 0.4) MHz	(104 ± 7) MHz
Stabilized beat note (fig. 5.6(a))	1 kHz	(1.71 ± 0.05) kHz	(1.99 ± 0.02) kHz
Stabilized beat note (HR) (fig. 5.6(b))	1 Hz	(6.4 ± 0.7) Hz	(6.0 ± 0.3) Hz

Figure 5.5: Beat note unlocked with voigt fit

(a) Beat note locked

(b) Beat note measured with highest resolution of Spectrum analyzer.

Figure 5.6: Locked beat note with different resolution

In order to test the long time duration of the laser stability, I measured the signal of the piezo feedback with a PicoLog that measures the voltage of the slow feedback every 60 ms. As shown in figure 5.7 the feedback-loop was able to make small corrections due to temperature drifts or other small disturbances in the laboratory for over 43.2 h. After that, a large disturbance can be seen in the measured data. This can either stem from a mode-hop or a bigger disturbance that the feedback-loop was not able to correct. Since the disturbance disrupted the stabilization of other lasers in the laboratory, one can assume that the stabilization of the slave laser was disturbed by a larger external factor in the laboratory. All in all the phase-offset frequency stabilization of the slave laser worked well over 43.2 h making the setup successful. The stabilized laser can now be used for further experiments.
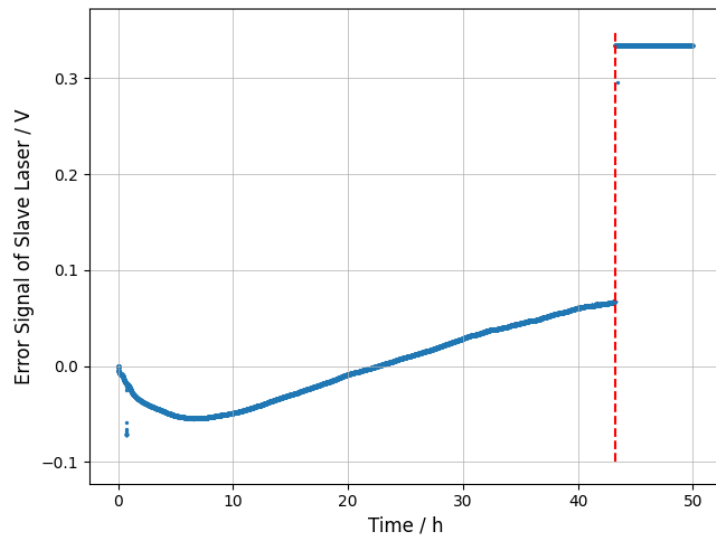
Figure 5.7: Long time measurement of piezo feedback. Duration of stabilized piezo feedback loop was approximately 43.2 h.

Conclusion

In this thesis, I was able to phase-offset frequency stabilize a high power diode laser to a free-running high power diode laser by building a feedback loop. These high power lasers can be later used to further optimize the setup of the YQO experiment in multiple ways.

In order to build the feedback loop I first setup both lasers and measured the laser thresholds and the beam profiles of the lasers. To be able to tune the lasers to the correct frequency, I adjusted the grating of both lasers and the current of the diode, the voltage applied to the piezo, and the temperature while ensuring the lasers are running nearly mode-hop free.

Then, I optically overlapped both laser beams. For that, I build the optical setup shown in figure 3.1. In order to optimize the overlap, I first ensured that the beam size of both beams was focused to the effective sensitive area of the photodiode using a beam profile camera. Then I measured the contrast of the overlapping beams with a PDA10A2 photodiode connected to an oscilloscope while ensuring that the power of both beams was similar. By improving this contrast from $V = (0.543 \pm 0.005)$ to $V = (0.609 \pm 0.004)$ I was able to improve the overlap of the lasers and thus measure the first beat notes using a fast photodetector and a spectrum analyzer.

After that, I build a setup which generates an error signal by comparing the beat note frequency and a reference frequency given by a DDS Arduino board. Furthermore, I measured the decrease of the beat note amplitude for higher frequencies, as the evaluation board cannot properly process signals of small amplitudes. To be able to frequency stabilize the laser to higher phase offsets, one could use gain equalizers.

Finally, I setup a dual-feedback loop consisting of a current and a piezo feedback loop. As a PID regulator I used the FALC pro and adjusted its overall gain. By measuring the error signal of the current and the piezo feedback I was able to optimize the parameters of the PID regulator. To verify the stabilization of the slave laser, I measured the linewidth of the beat note peak. Furthermore, I measured the error signal of the piezo feedback in order to then confirm the duration of the feedback loop. With the optimized parameters of the PID regulator, the feedback loop was able to phase-offset frequency stabilize the laser over 42 h, showing that the setup was successful.

Bibliography

[1] D. Meschede, *Optics, light and lasers: the practical approach to modern aspects of photonics and laser physics*, eng, 2nd. rev. and enl. ed., Physics textbook, Weinheim: Wiley, 2007, ISBN: 352740628X.

[2] W. Demtroder, *Laser spectroscopy.: (Basic principles)*, eng, Fifth edition., vol. 1, Springer, 2014, ISBN: 9783642538582.

[3] X. Wang et al., *Two-color ytterbium magneto-optical trap in a compact dual-chamber setup*, Phys. Rev. Appl. **23** (1 2025) 014004, URL: https://link.aps.org/doi/10.1103/PhysRevApplied.23.014004.

[4] J. Appel, A. MacRae and A. I. Lvovsky, *A versatile digital GHz phase lock for external cavity diode lasers*, Measurement Science and Technology **20** (2009) 055302, URL: https://dx.doi.org/10.1088/0957-0233/20/5/055302.

[5] *Evaluation Board User Guide UG-158*, Available at https://www.analog.com/media/en/technical-documentation/user-guides/UG-158.pdf (visited on 09.01.25), Analog Devices, 2010.

[6] O. Svelto, *Principles of Lasers*, eng, 5th ed., Netherlands: Springer Nature, 2010, ISBN: 9781441913029.

[7] *Tunable Diode Lasers*, Available at https://www.toptica.com/fileadmin/Editors_English/11_brochures_datasheets/01_brochures/toptica_BR_Scientific_Lasers.pdf (visited on 14.01.25), TOPTICA Photonics, 2018.

[8] C. E. Wieman and L. Hollberg, *Using diode lasers for atomic physics*, Review of Scientific Instruments **62** (1991) 1.

[9] E. Hecht, *Optik*, Berlin, Boston: De Gruyter Oldenbourg, 2023, ISBN: 9783111025599, URL: https://doi.org/10.1515/9783111025599.

[10] *Anamorphic Prism Pairs*, Available at https://www.thorlabs.com/newgrouppage9.cfm?objectgroup_id=149(visited on 15.01.25), Thorlabs.

[11] *UltrafastMSM photodetectorsG4176series(GaAs)*, Available at https://www.datasheets360.com/pdf/-5073308062623184073 (visited on 15.01.25).

[12]   *Data Sheet - ADF4007*, Available at `https://www.analog.com/media/en/technical-documentation/data-sheets/ADF4007.pdf`(visited on 09.01.25), Analog Devices, 2012.

[13]   *Coaxial Amplifiers - ZX60-6013E-S+*, Available at
`https://www.minicircuits.com/pdfs/ZX60-6013E-S+.pdf` (visited on 17.01.25),
Mini-circuits.

[14]   K. H. Ang, G. Chong and Y. Li, *PID control system analysis, design, and technology*,
IEEE transactions on control systems technology **13** (2005) 559.

[15]   *FALC pro*, Available at `https://www.toptica.com/products/laser-rack-systems/laser-locking-electronics/falc-pro` (visited on 09.01.25),
TOPTICA Photonics.

[16]   M. Chen, Z. Meng, J. Wang and W. Chen,
Ultra-narrow linewidth measurement based on Voigt profile fitting, Opt. Express **23** (2015) 6803,
URL: `https://opg.optica.org/oe/abstract.cfm?URI=oe-23-5-6803`.

[17]   P. Parkprom, N. Chattrapiban, P. Sompet and N. Thaicharoen,
Laser linewidth measurement using beat-note technique,
Journal of Physics: Conference Series **2653** (2023) 012081,
URL: `https://dx.doi.org/10.1088/1742-6596/2653/1/012081`.

Acknowledgments

First I would like to thank Prof. Hofferberth for giving me the opportunity to write my Bachelor thesis in the NQO group. I would like to thank Dr. Vewinger for being the second appraiser of this thesis.

A special thanks goes to Tangi as the supervisor of this thesis for the support throughout the experimental part of the thesis as well as the writing part. Moreover, I would like to thank the members of the YQO/FYQO group: Florian, Xin, Eduardo, Mengna, Ludwig and Knut for showing me around the lab, answering questions and kindly welcoming me into the group.
Thanks as well to the whole NQO group for the nice work atmosphere including the lunch and coffee breaks.

Furthermore, I would like to thank my family and my friends, especially Anna Witte and Kathrin Schumacher, for the emotional support throughout the process of writing this thesis.